Manuscript

Numerical Investigation on the Effects of Tensioning on the Dynamic Performance of a Pantograph

Lucky Ugochukwu Adoh[a,b*], Lovejoy Mutwatiwa[a], Celestin Nkundineza[a]

[a]African Railway Center of Excellence, Addis Ababa Institute of Technology, Addis Ababa University, Addis Ababa, Ethiopia.

[b]Department of Mechanical Engineering, Federal University of Technology, Akure, Nigeria

Corresponding author: lucky.ugochuwkwu@aait.edu.et

ARTICLE INFO

Keywords:
Dynamic performance
Pantograph-catenary system
Tensioning force
Stiffness, Light Rail Transit

ABSTRACT

The aim of this analysis was to model the pantograph - catenary system at static equilibrium and provide analytical solutions by computing the natural frequencies of the system, mode functions, equivalent stiffness of the catenary system and the deflections of the catenary wire as a function of position, time and tensioning force. Furthermore, dynamic analysis was conducted analytically and the results of the dynamic performance were obtained. It was shown that the dynamic response of the catenary system is dependent on the design parameters in which tensioning force is included. It was also shown that low tensioning forces result in high risk of contact loss and increased wave propagation in the catenary wire while high tensioning forces result in increased static stresses in the catenary system. The results in this article can be used to select optimum tensioning forces and design parameters for desired pantograph-catenary dynamic performance for different applications.

1 Introduction

The use of light rail trains in Africa is increasing due to rapid population growth in cities and high rate of infrastructure development. This is also because of their numerous advantages over the conventional road vehicles. Light rail trains are very safe, reliable, sustainable, cheap, environmental friendly, convenient, and comfortable for passengers and they also enable mass transportation of people [1] – [3]. Most of the light rail trains are electric trains and they draw power from the overhead line electrification system via the pantograph [4]. As the pantograph slides against the catenary wire, friction is generated which leads to gradual wear of the pantograph as well as the contact wire [5]. The amount of friction force generated depends on the electric spark due to loss of pantograph contact and design parameters of the catenary system among which the tensioning force of the catenary wire is included [6]. The pantograph-catenary system dynamic behavior has been studied intensely by numerous researchers and prior studies have identified the effects of the catenary system parameters on the dynamic performance of the pantograph. Factors that affects the quality of current collection of the pantograph include the catenary stiffness variation in the overhead wire [7], the pantograph stiffness, the rail vehicle speed, the pantograph uplift force, fluctuations of the contact force and the propagated flexural wave motion in the overhead wire etc. [8]. To ensure high quality current collection of the pantograph, reduced rate of overhead wire wear, reduced risk of arcing and increased lifespan, the catenary system parameters must be optimized [9]. The performance of an electric train mainly depends on the quality of current collection of the pantograph [10]. Different approaches and methodologies have been presented by various scholars on how to use analytical techniques to optimize the parameters of the pantograph-catenary system so as to reduce maintenance and operational cost, boost the revenues of the rail industry and increase its competition as well as its market share in the transportation industry. Hyeon and Kim [11] investigated the influence of contact wire pre-sag on the dynamics of the pantograph catenary system. Garcia [12] studied the effects of the catenary system stiffness on the contact force variation and he concluded that a high catenary stiffness reduces the contact force variation and improve the quality of pantograph current collection. Another researcher [13] investigated dynamic performance and parameter optimization of pantograph-catenary system and he proved that the dynamic performance depends on the speed of the rail vehicle apart from other factors. Taylor [14] modelled the pantograph-catenary system as a time-varying, single degree-of-freedom system to facilitate an analytical investigation of the system dynamics and he used the finite element method to determine the catenary characteristics and Floquet theory to analyze the behavior of the coupled system. They concluded that to achieve better current collection quality the head of the pantograph should be made as light as possible and the average stiffness of the catenary should be high.

A more overarching approach to the optimization of a single parameter of the catenary system and a comprehensive evaluation on its effect on the dynamic performance is not identified in most past researches. Therefore a single parameter (i.e. catenary tensioning) is going to be investigated in this paper and its effects on wear and pantograph-catenary dynamics are presented. The dynamic performance of a pantograph highly depends on the catenary system stiffness which in turn highly depends on the catenary tensioning [15]. It is crucial to gain an insight in recent investigation on the pantograph-catenary dynamic performance. Wu and Brennan

[16] investigated the dynamic response of a single degree of freedom coupled catenary pantograph system by evaluating the dynamic stiffness of the catenary system as the contact force divided by the vertical displacement caused by that particular force at a certain point in time. Their analysis provided a basic understanding of the interaction between the pantograph and the catenary system and it showed that the dynamic performance of the pantograph-catenary system highly depends on the catenary dynamic stiffness which is a function of tensioning force and catenary span length. Increasing the tension results in increased catenary stiffness as well as the stresses acting on the catenary system. Therefore there is need to optimize the catenary tensioning force to best suit the operation condition of a particular railway line. To focus on the investigated parameters a variety of pantograph models have been presented by many researchers. In most cases, the true physical structure and behavior of the pantograph are neglected. Benet and Alberto [17] modeled the pantograph as two string mass system without damping and they took into consideration the stiffness between the contact surfaces (i.e. the pantograph pan-head and the catenary conductor). Kumaniecka [18] identified the pantograph as a three mass system with four degrees of freedom. A pantograph model to be adopted in this paper has been presented by [19] which identify a pantograph as a three degree of freedom mass-spring system with damping and stiffness between the contact surfaces. To obtain the response of the coupled pantograph catenary system a range of methods are available. A researcher in [16] used the Fourier transform using the Floquet's theory to obtain the steady state response of a single degree of freedom couple pantograph-catenary system. Taylor [14] obtained the free vibration modes of the overhead wire system and the contact force using the Reyleigh-Ritz and modal analysis methods, respectively. Another coupled pantograph-catenary system was analyzed and solved by [12] using a fourth-order Runge–Kutta method taking into account Kuhn–Tucker conditions. All these methods showed that even though analytical methods are sophisticated and at some point cumbersome, they provide an in depth understanding of the basic interaction between a tensioned, spring supported string subjected to a periodic dynamic load. The same approach as presented by previous researchers will be used in this paper.

A full analysis of the pantograph-catenary system from one mast to another results in nonlinear equations of motion because of the variation of the catenary parameters across droppers. The variations in the catenary stiffness and tensioning is very small in-between dropper that it can be neglected and these parameters can be assumed as constants, but as we over pass a dropper the variation in these parameters is significant that it can't be neglected. To simplify the analytical analysis of the coupled pantograph-catenary system most of the above mentioned researchers analyzed the motion of the pantograph in-between two droppers where the catenary parameters and properties are constant and the governing equations of the physical system are linear. Analytical methods are not as efficient as software packages in solving nonlinear governing equations of a full catenary system. To cater for the nonlinearity of the dynamics of the pantograph-catenary system due to variations in parameters, the Finite Element Approach (FEA) is adopted by researchers [20] to have an in-depth understanding of the catenary system response due to variations in parameters.

Zhou and Zhang [13] used the finite element method and time integration method to solve the coupled equation of motion for the pantograph and the catenary system. Their aim was to find an optimal design of catenary and pantograph system by analyzing the influence of different design parameters on the dynamic performance. Using the FEA model their conclusion was that the dynamic performance of the pantograph-catenary system highly depends on the design parameters, including the stiffness and damping of the pan-head and frame, the static uplift force and the tension of the contact wire. They showed that to avoid contact loss between the contact wire and the pantograph at high train speeds the catenary tension must be increased. This is true for the improvement of the quality of current collection but increased tension force means increased stresses in the catenary wire and this might increase the rate of wear and reduce the lifespan of the catenary system leading to high maintenance costs and possibly losses.

This paper aims on identifying the optimal tensioning force in the catenary system used in light rail transits. A comprehensive evaluation of a single parameter of the catenary system is going to be provided which is not identified my most recent studies on the dynamic performance of the pantograph catenary system. An analytical solution for the catenary vertical displacement due to the contact force is going to be provided using the orthogonality principle. The catenary stiffness is described as a ratio of the contact force to the catenary vertical displacement.

2 Catenary system

A catenary system consists of components put together to supply electric current to the train via a pantograph(a device mounted on electric locomotives which is used to collect electric current from overhead line electrification system for moving trains) sliding on the contact wire. The quantity of current supplied to the train is determined by the quality of contact between the pantograph and the catenary wire [18]. High contact forces can cause excessive wear on the sliding surfaces, while too weak forces may lead to contact losses and sparking, which apart from the catenary and pantograph damage it can interrupt the energy supply to the train.

2.1 Catenary-Pantograph model

The pantograph is modeled as a spring-mass system consisting of the contact strip and the lower and the upper frames. The uplift force due to the pantograph hydraulic system, the aerodynamic forces due to wind and the contact force were taken into consideration in this study. The pantograph moved at a constant velocity of *120 km/h*. The contact wire is suspended from the messenger wire by the droppers, and the messenger wire hangs directly on the supports at each end of the span. The contact wire is modeled as a thin Euler-Bernoulli beam [22] having bending stiffness EI and a constant tensioning force T, in between the mast and L is the distance between the two masts as shown in Fig. 1 below. To simplify the model, the following assumptions were made for the catenary system;

- The catenary wire system is assumed to be a beam under vertical vibration.
- The catenary wire is model as a thin Euler-beam with pre-tensioned force.
- The contact wire is modeled between two droppers.

- The beam is subjected to bending due to contact force.
- The pantograph contact force is in vertical direction upwards.
- The displacement of the catenary wire is only in the vertical direction.

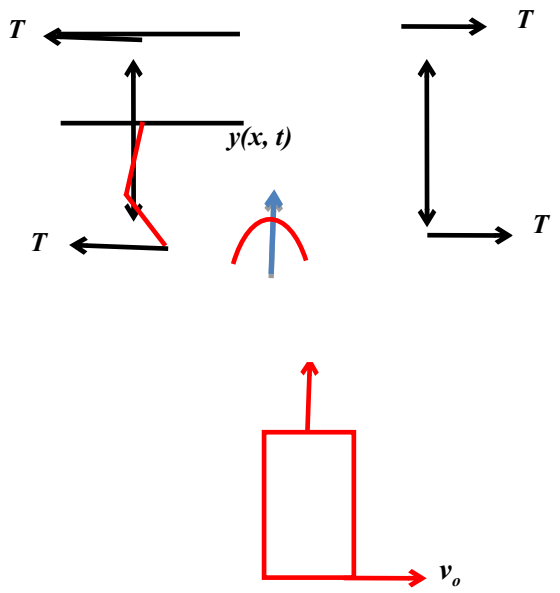

Fig. 1. Catenary-Pantograph model

$y(x,t)$ is the vertical displacement of the catenary wire.
T is the tensioning forces.
$P(x,t)$ is the pantograph contact force.
v_0 is the velocity of the train.
The inertia force is given by;

$$I(x,t)=\rho A dx\frac{dy(x,t)}{dt^2}, \tag{1}$$

where $\rho \wedge A$ are the contact wire material density and the cross sectional area respectively. *dx* is an infinitesimal length along the longitudinal length of the catenary system.
The governing equation of the catenary contact system is defined as:

$$\frac{\partial^2}{\partial x^2}\left[EI\frac{\partial^2 y}{\partial x^2}\right]+\rho A\frac{\partial^2 y}{\partial t^2}-T\frac{\partial^2 y}{\partial x^2}=f(x,t), \tag{2}$$

where $f(x,t)$ is the summation of all external force acting on the catenary contact wire and it consist of

- Gravitational force, mg which is assumed to be negligible in this study since the mass in contact wire at the point of contact with the pantograph is very small relative to the masses of the pantograph upper and lower frames.
- Contact force, $P(x,t)$.
- Aerodynamic force.
- Pantograph uplift force.

To fully understand the dynamic behavior of the catenary-pantograph system the governing equation of the system i.e. Eq. (2) was solved analytically taking into consideration two scenarios. First, the free vibration condition was considered to obtain the natural frequencies and mode shapes of the catenary system. Second, the forced vibration condition was considered to compute the dynamic response of the pantograph-catenary system which is in terms of the catenary vertical displacements and is denoted by $y(x,t)$.

2.2 Catenary system modal analysis

Under free vibration the governing equation is written as:

$$\frac{\partial^2}{\partial x^2}\left[EI\frac{\partial^2 y}{\partial x^2}\right]+\rho A\frac{\partial^2 y}{\partial t^2}-T\frac{\partial^2 y}{\partial x^2}=0. \tag{3}$$

Apply the separation of variables technique; the free vibration response can be assumed as:

$$y(x,t)=\sum_{n=1}^{\infty}Y_n(x)\left(A_n\cos\omega_n t+B_n\sin\omega_n t\right) \tag{4}$$

where $Y_n(x)$ is the contact wire spatial amplitude of vibration corresponding to the n^{th} mode and ω_n is the natural frequency of vibration of the contact wire corresponding to n^{th} mode of vibration.
Substituting Eq. (4) into Eq. (3) yields:

$$\begin{aligned}&EI\frac{\partial^4 Y_n}{\partial x^4}\left(A_n\cos\omega_n t+B_n\sin\omega_n t\right)\\&-T\frac{\partial^2 Y_n}{\partial x^2}\left(A_n cos\omega t+B_n sin\omega t\right)\\&+\rho A\frac{\partial^2\left(A_n cos\omega t+B_n\sin\omega_n t\right)}{\partial t^2}=0\end{aligned} \tag{5}$$

Eq. (5) can be reduced into

$$\frac{d^4 Y_n}{dx^4}-\frac{T}{EI}\frac{d^2 Y_n}{dx^2}-\frac{\rho A}{EI}\omega_n^2 Y_n=0, \tag{6}$$

The solution of ODE in Eq. (6) is given by

$$\begin{aligned}&Y_n(x)=C_1\cosh(r_1 x)+C_1\sinh(r_1 x)\\&+C_3\cos(r_2 x)+C_4\sin(r_2 x),\end{aligned} \tag{7}$$

where $r_i, for\, i=1,2$ is given by:

$$r_1^2, r_2^2=\frac{T}{2EI}\pm\sqrt{\frac{T^2}{4E^2I^2}+\frac{\rho A\omega^2}{EI}}; \tag{8}$$

and r_i is obtained by solving the resulting frequency characteristic equation from Eq. (6).
The boundary conditions of a simply supported beam are:

$$@x=0;Y(0)=0;\frac{d^2Y(0)}{dx^2}=0. \quad (9)$$

$$@x=L;Y(L)=0;\frac{d^2Y(L)}{dx^2}=0. \quad (10)$$

Applying the boundary conditions in Eq. (10) we obtain the values of r_1 and r_2 :

$$Y(x)=C_2\sinh(r_1x)+C_4\sin(r_2x), \quad (11)$$

$$\frac{C_2}{C_4}=\frac{-\sin r_2L}{\sinh r_1L}, \quad (12)$$

$$\sinh r_1L\neq 0, \quad (13)$$

$$-\sin r_2L=0, \quad (14)$$

$$r_2L=arc\sin 0+\pi n,$$
$$r_2=\frac{\pi n}{L},n=1,2,3,\ldots, \quad (15)$$

$$Y_n(x)=C_n\left[\frac{-\sin r_2L}{\sinh r_1L}\sinh(r_1x)+\sin(r_2x)\right], \quad (16)$$

whereC_n is the vibration mode constant.

Eq. (16) is defined as the mode function or the normal function of the n^{th} mode of vibration. Recalling that the natural frequencies of the catenary are evaluated as follows:

$$\left(\frac{n\pi}{l}\right)^2=\frac{T}{2EI}-\sqrt{\frac{T^2}{4E^2I^2}+\frac{\rho A\omega_n^2}{EI}}. \quad (17)$$

Solving forω_n, we have;

$$\omega_n=\frac{\pi^2}{L^2}\sqrt{\frac{EI}{\rho A}}[n^4+\frac{L^2n^2T}{EI\pi^2}]^{\frac{1}{2}}. \quad (18)$$

Eq. (18) corresponds to the natural frequencies of the n^{th} mode of vibrations.

2.3 Catenary system dynamic response

The contact wire is modeled as a simply supported Euler-Bernoulli beam subjected to a moving contact load from the pantograph. The contact force is not a constant, it varies due to variations in aerodynamic forces, catenary tensioning force and train speeds. To capture the real physical behavior of the contact force it is assumed there is a concentrated harmonic force at a certain point on the contact wire and in time [23].

$$P(x,t)=f_0 sin\omega t\sin\frac{n\pi x}{L}, \quad (19)$$

where

$L\,is$ length of the beam between the two masts,

x is the position of moving force,

ω is the forcing frequency,

f_0 is the force amplitude,

The governing equation of the Euler Bernoulli beam will result into:

$$EI\frac{\partial^4y}{\partial x^4}-T\frac{\partial^2y}{\partial x^2}+\rho A\frac{\partial^2y}{\partial t^2}=f_0 sin\omega t\sin \quad (20)$$

A variety of methods have been used to obtain the solution of a forced vibration Euler Bernoulli beam partial differential equation. A paper in A.I.N. Press [24] presented the solution of a Forced vibration Euler–Bernoulli beams by means of dynamic Green functions. In this study the orthogonality concept was used. From the free vibration solution presented above, the response of the system is given by:

$$y(x,t)=\sum_{n=1}^{\infty}c_n\sin\left(\frac{n\pi x}{L}\right)(Acos\,\omega_nt+Bsin\omega \quad (21)$$

Because the beam is subjected to a harmonically varying load we assume the particular solution of the governing equation Eq. (20) to be harmonic as well and take the form as:

$$y(x,t)=\sum_{n=1}^{\infty}a_nY_n\sin\left(\frac{n\pi x}{L}\right)\sin\omega t, \quad (22)$$

where ω is the same as the forcing frequency.

Differentiating Eq. (21) and substituting one mode corresponding particular solution into the governing equation we obtain:

$$EI\,a_n\left(\frac{n\pi x}{L}\right)^4\sin\left(\frac{n\pi x}{L}\right)\sin\omega t+T\,a_n\left(\frac{n\pi x}{L}\right)^2\sin$$
$$-\rho A\,a_n\omega^2\sin\left(\frac{n\pi x}{L}\right)\sin\omega t=f_0 sin\omega t\sin\left(\frac{n\pi x}{L}\right. \quad (23)$$

Simplifying further,

$$EI\,a_n\left(\frac{n\pi x}{L}\right)^4+T\,a_n\left(\frac{n\pi x}{L}\right)^2-\rho A\,a_n\omega_n^2=f_0. \quad (24)$$

We now have:

$$a_n=\frac{f_0}{EI\left(\frac{n\pi x}{L}\right)^4+T\left(\frac{n\pi x}{L}\right)^2-\rho A\,\omega^2}. \quad (25)$$

The forced vibration solution for Euler Bernoulli beam then becomes:

$$y_n(x,t)=\sum_{n=1}^{\infty}c_n\sin\left(\frac{n\pi x}{L}\right)(A_n\cos\omega_nt+B_n\sin\omega_nt)$$
$$+a_n\sin\left(\frac{n\pi x}{L}\right)\sin\omega t.$$

(26)

Applying the initial conditions to Eq. (26);

$$y(x,0)=0,\frac{\partial Y(x,0)}{\partial t}=0,c_n=1, \tag{27}$$

$$y(x,t)=\sum_{n=1}^{\infty} a_n \sin\left(\frac{n\pi x}{L}\right)\left(\sin\omega t-\frac{\omega}{\omega_n}\sin\omega_n t\right). \tag{28}$$

The expression of $y(x,t)$ defined so far is due to a harmonic contact force at a particular point on the catenary. To transform the load into a moving force we conduct Fourier transform [22] by defining the point load, *P* as a distributed load *f(x)* over a small finite interval $2\Delta x$ where P is at the middle.

$$f(x)=\begin{cases} 0, 0<x<d-\Delta x \\ \dfrac{P}{2\Delta x}, d-\Delta x<x<d+\Delta x, \\ 0, d+\Delta x<x<L \end{cases} \tag{29}$$

where *d* is the distance from the starting point to the point where the force is acting on, and *L* is the length of the beam. Using *sine* Fourier transformation and defining:

Transformation and defining f_n from the given *f(x),* we can write;

$$f_n=\frac{2}{L}\int_{d-\Delta x}^{d+\Delta x}\frac{P}{2\Delta x}\sin\left(\frac{n\pi x}{L}\right)dx=\frac{P}{L\Delta x}\left[\frac{-L}{n\pi}\cos \tag{30}$$

$limits¿ d-\Delta x ¿ d+\Delta x,$

$$f_n=\frac{2P}{L}\left[\sin\left(\frac{n\pi d}{L}\right)\frac{\sin\left(\frac{n\pi\Delta x}{L}\right)}{\frac{n\pi\Delta x}{L}}\right]. \tag{31}$$

Taking the limit as Δx approaches *0*, we can write:

$$f_n=\frac{2P}{L}\left[\sin\left(\frac{n\pi d}{L}\right)\lim_{\Delta x\to 0}\frac{\sin\left(\frac{n\pi\Delta x}{L}\right)}{\frac{n\pi\Delta x}{L}}\right]=\frac{2P}{L}\sin \tag{32}$$

where

$d=v_0 t$; and,
d is the position of the moving force,
v_0 the velocity of the moving force, and
t the time.

Modifying Eq. (28) by substituting in $\omega=\frac{n\pi v_0}{L}$, the response of the catenary wire subjected to a moving load becomes:

$$y(x,t)=\sum_{n=1}^{\infty} a_{fn}\left[\sin\left(\frac{n\pi v_0}{L}t\right)-\frac{\omega}{\omega_n}\sin(\omega_n t)\right], \tag{33}$$

where

$$a_{fn}=\frac{\frac{2P}{L}\sin\left(\frac{n\pi x}{L}\right)}{EI\left(\frac{n\pi x}{L}\right)^4+T\left(\frac{n\pi x}{L}\right)^2-\rho A\left(\frac{n\pi v_0}{L}\right)^2}.$$

Defining the catenary equivalent dynamic stiffness *K* as:

$$K=\frac{P}{y_n(x,t)}, \tag{34}$$

$$K=\sum_{n=1}^{\infty}\frac{EI\left(\frac{n\pi x}{L}\right)^4+T\left(\frac{n\pi x}{L}\right)^2-\rho A\left(\frac{n\pi v_0}{L}\right)^2}{\frac{2}{L}\sin\left(\frac{n\pi x}{L}\right)\left[\sin\frac{n\pi v_0}{L}t-\frac{\omega}{\omega_n}\sin\omega_n t\right.} \tag{35}$$

3 Pantograph modal analysis

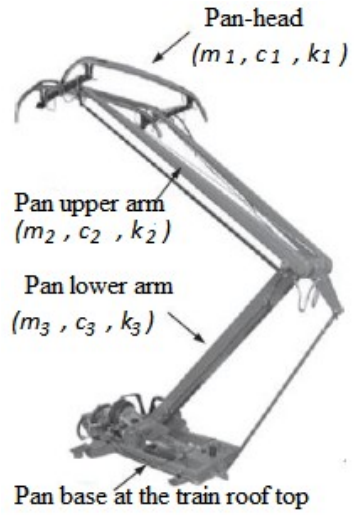

(a)

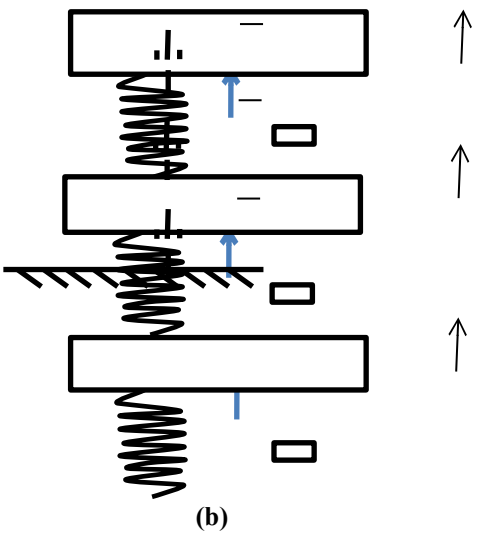

(b)

Fig. 2. (a) Pantograph physical model [10]. **(b)** Pantograph mathematical model.

The physical parameters of the pantograph represented by Fig. 2 are described here below:

Pan-head mass: m_1 = *7.5 1kg,*
Upper arm mass*:* m_2 = *5.855 kg,*
Lower arm mass*:* m_3 = *4.645 kg,*
Pan head damping constant*:* c_1 = *0 N.s/m,*
Upper arm damping constant: c_2 = *0 N.s/m,*
Lower arm: c_3 = *70 N.s/m,*
Pan-head stiffness*:* k_1 = *8380 N/ m,*
Upper arm stiffness: k_2 = *6200 N /m,*
Lower arm stiffness: k_3 = *80 N/ m,*
Uplift force at the base of the pantograph: F_0 = *70 N,*
Aerodynamic force on upper arm: F_1 = *120 N,*
Average pan head-catenary contact force: F_c = *50 N.*

From Fig. 2 of the pantograph model, the equations of the pantograph is given as

$$\begin{aligned} &m_1\ddot{x}_1+c_1\dot{x}_1-c_1\dot{x}_2+(k_1)x_1-k_1x_2=F_c,\\ &m_2\ddot{x}_2-c_2\dot{x}_3-c_1\dot{x}_1+(c_1+c_2)+(k_2+k_1)x_2-k_1 \\ &m_3\ddot{x}_3-c_2\dot{x}_2+(c_3+c_2)\dot{x}_3+(k_2+k_3)x_3-k_2x_2= \end{aligned} \quad (36)$$

Considering the free un-damped vibration of the pantograph we can write:

$$\begin{bmatrix} m_1 & 0 & 0\\ 0 & m_2 & 0\\ 0 & 0 & m_3 \end{bmatrix}\begin{Bmatrix} \ddot{x}_1\\ \ddot{x}_2\\ \ddot{x}_3 \end{Bmatrix}+\begin{bmatrix} k_1 & -k_1 & 0\\ -k_1 & k_1+k_2 & -k_2\\ 0 & -k_2 & k_2+k_3 \end{bmatrix}\begin{Bmatrix} x_1\\ x_2\\ x_3 \end{Bmatrix}=\begin{Bmatrix} 0\\ 0\\ 0 \end{Bmatrix}. \quad (37)$$

Assuming

$$\begin{aligned} x_i(t)&=X_i\cos(\omega t+\theta_1)\wedge¿\\ \ddot{x}_i(t)&=-X_i\omega^2\cos(\omega t+\theta_1)\,for\,i=1;2;3. \end{aligned} \quad (38)$$

and performing substitution into Eq. (37) we get:

$$ZX=0, \quad (39)$$

where

$$Z=¿$$

and

$$X=\begin{Bmatrix} X_1\\ X_2\\ X_3 \end{Bmatrix}.$$

The natural frequencies of the pantograph are obtained from the eigenvalues of the matrix **Z**.

$$\omega^2{}_1=4.4$$
$$\omega^2{}_2=1246.8$$
$$\omega^2{}_3=3706.8$$

The corresponding modes of vibration are obtained from the eigenvector:

$$\omega_1=2.0976\,modes=\begin{bmatrix} -0.5807\\ -0.5784\\ -0.5729 \end{bmatrix},$$

$$\omega_2=35.31\,modes=\begin{bmatrix} -0.5562\\ 0.0653\\ 0.8285 \end{bmatrix}.$$

$$\omega_3=60.88\,modes=\begin{bmatrix} -0.3508\\ 0.8147\\ -0.4618 \end{bmatrix},$$

4 Discussion

The analysis was conducted in between two masts. A contact force moving at a constant speed of *120 Km/h* was used to determine the dynamic behavior of the catenary. To analyze the effects of tensioning on the dynamic performance of the pantograph-catenary system, the equivalent dynamic stiffness of the catenary was determined by dividing the dynamic response of the catenary system by the contact force at a particular position in time. Therefore, prior to investigating the effects of tensioning on dynamic performance of the catenary-pantograph system, the dynamic response of the catenary system due to a moving force was studied. The natural frequencies of the catenary system corresponding to different tensioning forces ranging from *15 KN* to *35 KN* and also corresponding to different modes from mode *1* to *6* are shown in the Figure 3.

To observe the behavior of the natural frequencies at different tensioning forces, increments of *4 KN* were given for each mode and the natural frequencies were calculated for the *6* modes. As it can be seen from the Fig. 3 above, that the natural frequencies increase as the tensioning force increases. Increased natural frequencies result in increased structural stiffness which reduces the displacement of the catenary in the vertical direction but increases the wear between the sliding surfaces due to increases system static stresses. A plot of natural frequencies against tensioning forces as shown in Fig. 3, there is a linear relationship between tensioning forces and natural frequencies. This insight gives a picture of the nature of an optimum tensioning force range. In the methodology, the natural frequencies of the pantograph were calculated. An optimum tensioning value should provide natural frequencies of the catenary at all modes far away from the natural frequencies of the pantograph to avoid resonance and improve stability. Between tensioning values of *15 KN* and *23 KN* the natural frequencies of the catenary are within the same range as that of the pantograph which means catenary tensioning values within the *15 KN-23 KN* range increases the risk of resonance which is unacceptable due to its adverse effects on the dynamic performance of that catenary-pantograph system. A plot of dynamic stiffness against tensioning force is shown in Fig. 5.

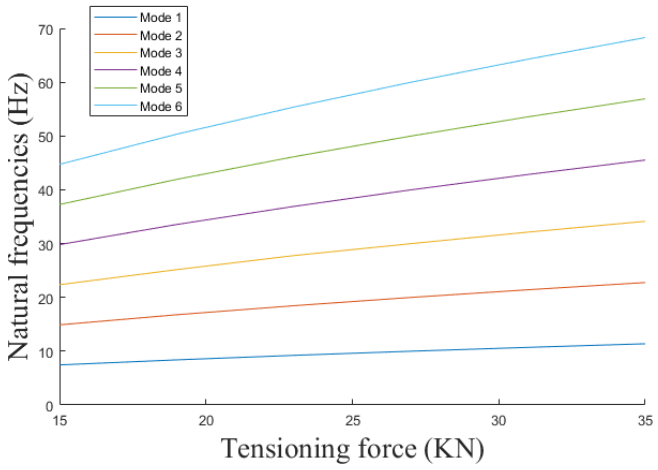

Fig. 3. Fundamental natural frequencies against tensioning forces

4.1 Dynamic stiffness of the catenary system

As it can be observed from Fig. 4, the catenary stiffness has its highest value near the supports (i.e. @ *x=10 m* and @ *x=40 m*) this fact is because on practical grounds the contact wire is fixed to the masts at both ends and the stiffness is high due to the rigidity of the masts. The stiffness against position graph is a parabolic curve with its minimum at the middle of the span. This behavior is expected because the catenary is loose at the middle of the span as compared to the ends. Therefore it is expected that the deflection of the catenary in the vertical direction will be high as the pantograph moves. The catenary tensioning forces ranges from *15 KN* to *35 KN* and the catenary stiffness behaves in a wave form as the tensioning force increases.

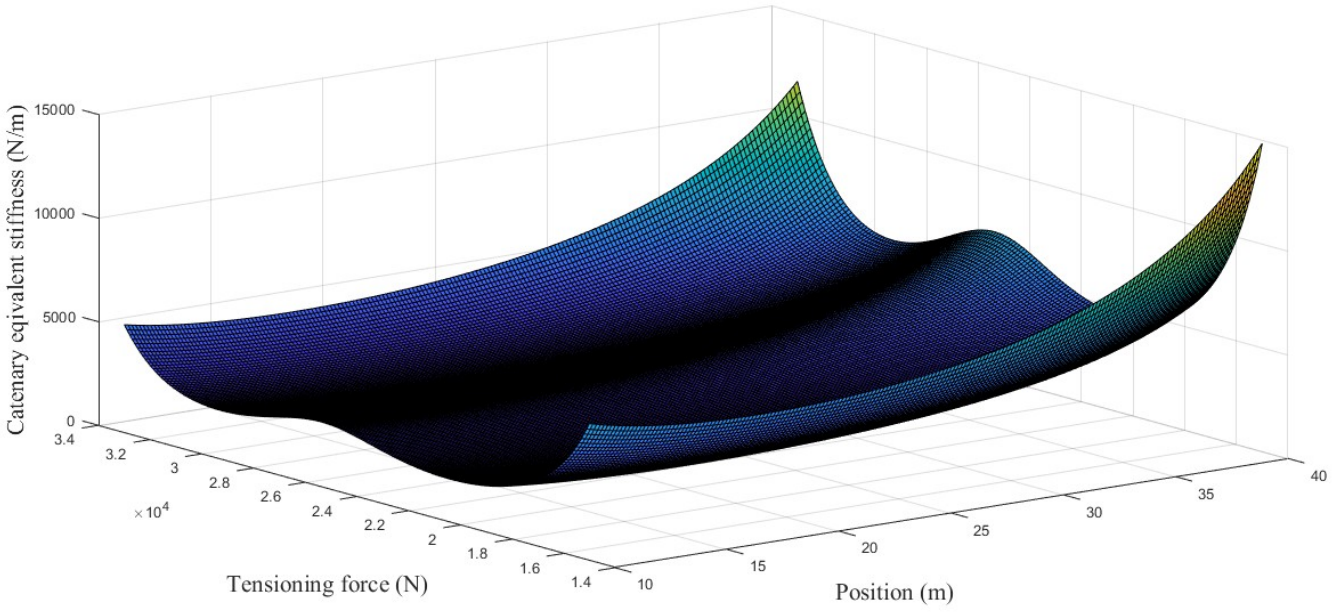

Fig. 4. Dynamic stiffness (N/m) of the catenary wire in a span at various tensioning forces (N)

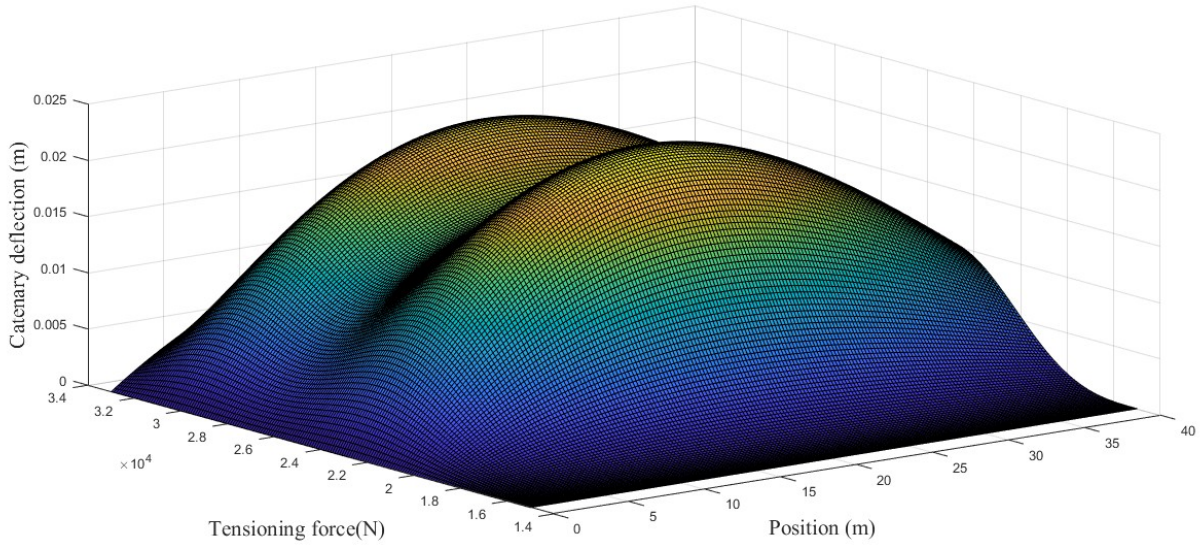

Fig. 5. The dynamic response of the catenary contact wire due to a moving average contact force of *50 N*.

At a tensioning value of *15 KN* and at *x=10 m* the catenary stiffness is high and decreases as the tension increases. At tensions between *18 KN* and *20 KN* the stiffness reaches its minimum and gradually increases again. At the middle of the specified range of the tensioning force value the catenary reaches a peak value that is lower than the catenary stiffness at the ends. As observed from the graph the catenary stiffness behaves the same way with tensioning force as the pantograph moves from one end of the span to another.

Increasing the contact force results in an increase in the catenary vertical displacements as it has been demonstrated in the Fig. 5. A maximum deflection when a contact force of *100 N* is used is *42 mm* while when a force of *50 N* is used the deflection is *20 mm*. The normal average contact force on practical grounds is *50 N*.

5 Conclusions

In conclusion to this work it has been addressed that the catenary system is subjected to various static and dynamic loads. The catenary is also subject to vibrations due to the movement of the pantograph or winds. The life span of an electric overhead system solely depends on the quality of the contact wire, messenger wire and droppers. The quality of these catenary system members depends on the degree of parameter optimization done on them. The whole focus of this study was to improve the quality of the catenary system through optimization of the tensioning force. The results indicated that increasing the tensioning force increased the stiffness of the catenary systems thereby reducing the vertical displacements of the contact wire. It means there is an increase in stability but the stresses acting on the catenary are

directly proportional to the tensioning force therefore there is a limit to how much the tensioning force will be set depending on the yield strength of the material used for the contact wire. Lower tensioning forces resulted in low stiffness values which increased the deflection of the catenary in the vertical sense and increased risk of resonance since the natural frequencies of the catenary coincide with those of the pantograph. Hence to improve the dynamic performance of the pantograph-catenary system according to the dimensions given in this study a range of tensioning force values from *24 KN* to *31 KN* was prescribed.

Acknowledgments
This work is supported by the African Center of Excellence project 2 (ACE II).

Declaration of Competing Interest
The authors declare that they have no known competing financial interests or personal relationships that could have appeared to influence the work reported in this paper.

Data availability
The raw/processed data required to reproduce these findings cannot be shared at this time due to legal or ethical reasons. The raw/processed data required to reproduce these findings cannot be shared at this time as the data also forms part of an ongoing study.

References

[1] L. U. Adoh, M. F. Akello, N. Faraja, and P. Ishimwe, "Prevention of Railway Accident using Arduino Based Safety System : A case Study of Addis Ababa Light Rail Transit," *international journal of engineering research & technology,* vol. 8, no. 09, pp. 327–332, 2019.

[2] L. U. Adoh, M. Lovejoy, and M. fiona Akello, "Safety Demonstration and Risk Management at Rail-Road Level Crossing at Addis Ababa Light Rail Transit Network," *International Journal of Scientific Research in Science, Engineering and Technology*, vol. 6, no. 5, pp. 103–109, 2019.

[3] F. M. Akello, L. U. Adoh, Simulation of Power Generation from Vibration of Railway Track, *International Journal of Sustainable and Green Energy*. Vol. 9, No. 1, 2020, pp. 16-22. doi: 10.11648/j.ijrse.20200901.12

[4] O. Lopez-garcia, A. Carnicero, V. Torres, and J. R. Jimenez-octavio, the influence of cable slackening on the stiffness computation of railway overheads "*International Journal of Mechanical Sciences,* ," vol. 50, pp. 1213–1223, 2008.

[5] S. Gregori, M. Tur, E. Nadal, F. J. Fuenmayor, and F. Chinesta, "Parametric model for the simulation of the railway catenary system static equilibrium problem," *Finite Element Analysis design,* vol. 115, pp. 21–32, 2016.

[6] T. Park, C. Han, and J. Jang, "Dynamic sensitivity analysis for the pantograph of a high-speed rail vehicle, *journal of sound and vibration*" vol. 266, pp. 235–260, 2003.

[7] Z. Liu, Measures to Enhance the Dynamic Performance of Railway Catenaries, *KTH Royal Institute of Technology*, urn:nbn:se:kth:diva-214464 ISBN 978-91-77295242, 2017

[8] J. Kim, H. Chae, B. Park, S. Lee, C. Han, and J. Jang, State sensitivity analysis of the pantograph system for a high-speed rail vehicle considering span length and static uplift force, *journal of sound and vibration*, vol. 303, pp. 405–427, 2007.

[9] A. Garcia, C. Gomez, R. Saa, F. Garcia-carballeria, and J. Carretero, "Optimizing the process of designing and calculating railway catenary support infrastructure using a high-productivity computational tool, Transportation Research Part C: Emerging Technologies, vol. 28, pp. 1–14, 2013.

[10] M. Arnold and B. Simeon, "Pantograph and catenary dynamics: A benchmark problem and its numerical solution, *applied numerical mathematics*, vol. 34, pp. 345–362, 2000.

[11] Y. Hyeon, K. Lee, Y. Park, B. Kang, and K. Kim, "International Journal of Mechanical Sciences Influence of contact wire pre-sag on the dynamics of pantograph – railway catenary," *International Journal of Mechanical Science*, vol. 52, no. 11, pp. 1471–1490, 2010.

[12] O. Lopez-garcia, A. Carnicero, and J. L. Maron, "Influence of stiffness and contact modelling on catenary – pantograph system dynamics, *journal of sound and vibration*, vol. 299, pp. 806–821, 2007.

[13] N. Zhou and W. Zhang, "Investigation on dynamic performance and parameter optimization design of pantograph and catenary system," *Finite Elem. Anal. Design*, vol. 47, no. 3, pp. 288–295, 2011.

[14] P. Taylor, "Vehicle System Dynamics: *International Journal of Basic Analytical Study of Pantograph-catenary System,Dynamics*,"doi.org/10.1080/00423119808969460. pp. 37–41, 2013.

[15] O. Lopez-garcia, A. Carnicero, and V. Torres, "Computation of the initial equilibrium of railway overheads based on the catenary equation,, *engineering structures*" vol. 28, pp. 1387–1394, 2006.

[16] A. No, "Dynamic stiffness of a railway overhead wire system and its effect on pantograph – catenary system dynamics, *journal of sound and vibration*" vol. 219, pp. 483–502, 1999.

[17] J. Benet, A. Alberto, E. Arias, and T. Rojo, "A Mathematical Model of the Pantograph-Catenary Dynamic Interaction with Several Contact Wires,"*International Journal of Applied Mathematics* vol.37 issue 2,p136-144. November, 2007.

[18] A. Kumaniecka, "Modelling and identification of catenary-pantograph system, *journal of theoretical and applied mechanics*," pp. 887–901, 2003.

[19] R. Unless, P. Act, W. Rose, T. If, and W. Rose, "This is a repository copy of Validation of a new model for railway overhead line dynamics . White Rose Research Online URL for this paper : Version : Accepted Version Article : Beagles , A ., Fletcher , D . orcid . org / 0000-0002-1562-4655 ," 2016.

[20] S. Gregori, M. Tur, E. Nadal, J. V Aguado, F. J. Fuenmayor, and F. Chinesta, "Fast simulation of the pantograph – catenary dynamic interaction," *Finite Element Analysis Design*., vol. 129, , pp. 1–13, January, 2017.

[21] P. Taylor, "Vehicle System Dynamics, *International Journal of Vehicle Mechanics and Mobility Pantograph / CatenaryDynamicsandControl*,"DOI:10.1080/00423119708969353, pp. 37–41, 1997.

[22] P. Taylor, C. N. Jensen, and H. True, "Vehicle System Dynamics : *International Journal of Vehicle Mechanics*

and Mobility dynamics of an electrical overhead line system," no., pp. 37–41,2014.

[23] C. Systems, S. S. Rao, and S. S. Rao, Vibration of Continuous. 2007 *John Wiley & Sons*, Inc. ISBN: 978-0-471-77171-5.

[24] A. I. N. Press, "Forced vibration of Euler – Bernoulli beams by means of dynamic Green functions, *journal of sound and vibration*" vol. 267, pp. 191–207, 2003.

[25] R. Ul, A. Uzzal, R. B. Bhat, and W. Ahmed, "Dynamic response of a beam subjected to moving load and moving mass supported by Pasternak foundation, *shock and vibration*" vol. 19, pp. 2